Calculation of self-energy matrices using complex absorbing potentials in electron transport calculations

J. A. Driscoll and K. Varga
Department of Physics and Astronomy, Vanderbilt University, Nashville, Tennessee 37235, USA
(Received 23 September 2008; revised manuscript received 26 November 2008; published 22 December 2008)

A method is presented to evaluate self-energy matrices used in the Green's function formulation of transport calculations. By adding a complex absorbing potential to the Hamiltonian of a semi-infinite lead, the problem of inverting an infinite-dimensional matrix is transformed into a finite-dimensional eigenvalue problem. The self-energies are calculated for all energies at once and can be tabulated for a given system. Examples are presented to show the accuracy of the approach.

DOI: 10.1103/PhysRevB.78.245118 PACS number(s): 73.40.−c, 73.63.−b, 72.10.−d, 85.65.+h

I. INTRODUCTION

Motivated by experimental advances, methods for quantum transport calculations have been developed at a great pace in the last few years. Quantum transport is naturally described within the nonequilibrium Green's function (NEGF) approach,[1–3] which allows the use of a many-body Green's function. However, the complexity of the problem limits the applicability to small systems. A more practical approach is to use the density-functional theory (DFT) Kohn-Sham Hamiltonian. The NEGF-DFT approach became a popular and widely used tool in quantum transport calculations,[4–15] but other approaches such as the Lippmann-Schwinger method[16] and the wave-function matching technique[17] have also been developed. The limitations and uncertainties of the NEGF-DFT calculations have also been studied (see, e.g., Ref. 18) and transport calculations based on time-dependent DFT (TDDFT) were proposed as a powerful alternative.[19,20]

Unlike conventional electronic structure calculations where one can use closed systems or periodic boundary conditions, in quantum transport calculations one has to deal with an open system where the device is connected to semi-infinite leads. The lead is usually built of periodically repeated blocks and the system can be divided into left lead, device (which may include several layers of the lead), and the right lead (Fig. 1). The transmission probability can then be calculated using a finite computational cell containing the device, provided that the boundary conditions are known on the surfaces dividing the device and the leads. These boundary conditions can be given either by the wave function or by the Green's function of the leads. The problem is that these boundary conditions have to be known at any energy for which $T(E)$ is to be calculated.

To calculate the transmission probability $T(E)$ within the NEGF formalism one first has to calculate the self-energies of the leads. Various methods have been developed for this purpose in the past. The common feature of these methods is that they have to be repeated for each energy of interest. The simplest method to calculate the Green's function of the lead is the iterative method, which is described, e.g., in Ref. 21. It starts with the calculation of the Green's function for a single block of the periodic lead and adds more and more blocks until convergence. The convergence however is extremely slow because the termination of the infinite lead at a finite distance generates reflections from the artificial boundary and this effect will only be negligible if the boundary is far away. The decimation method[22] is a clever variant of the iterative approach which greatly speeds up the convergence by increasing the lead in a recursive way. The decimation method is a very efficient way to calculate the Green's function of the lead and is used in many quantum transport codes. Other approaches calculate the Green's function by solving quadratic eigenvalue problems.[15,23,24] The review paper[21] gives a pedagogical introduction to these methods, shows the equivalence of the different approaches, and provides an extensive source of references of self-energy calculations.

Absorbing boundary conditions by using complex absorbing potentials (CAPs) were first introduced in time-dependent quantum-mechanical calculations to avoid artificial reflections caused by the use of finite basis sets or grids.[25] These CAPs are located in the asymptotic region and annihilate the outgoing waves preventing the undesired reflections. CAPs are intensively used in quantum-mechanical calculations of chemical reaction rates and in time-dependent wave-packet calculations.[26–34] Complex potentials have also been used in transport calculations.[35–37]

In this paper we show that a complex absorbing potential can be used as a very efficient tool to calculate the Green's function and the self-energy of the leads. As the self-energies are needed at many different energies, their calculation is often the dominant part of transport calculations. In the approach suggested in this paper one can obtain the self-energy for all energies at once. This is achieved by adding a CAP to the Hamiltonian of the leads. The CAP transforms the infinite lead into a finite system. The Hamiltonian of the lead then can be diagonalized and the Green's function can be

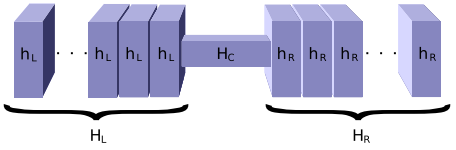

FIG. 1. (Color online) Schematic diagram of a two-probe device. The device is modeled by two semi-infinite electrodes (left and right) and a central region (c). The electrodes are divided into principal layers (blocks) that interact only with the nearest-neighbor layers.

calculated using a spectral representation for any energy.

In a sense our approach is the opposite of what the work in Ref. 37 pursued. In Ref. 37 a complex potential was derived approximately from the self-energies of the leads. The obtained complex potential was energy independent and nonlocal. By adding the derived complex potential to the Hamiltonian of the device the need for self-energies is bypassed, greatly simplifying the calculations. In this work we explicitly add a complex potential to the leads *to calculate* the energy dependent self-energy matrices. The energy dependence of the calculated self-energy matrices is simple and the computation associated with the leads is decoupled from the calculation of the device, just like in Ref. 37.

The outline of this paper is as follows. Section I is followed by the description of the approach in Sec. II. Numerical examples are presented in Sec. III followed by a summary and outlook.

II. METHOD

In this section first we briefly show the CAP and discuss its advantages. After introducing the definition of self-energy and transmission coefficient we will show how one can use the CAP to calculate the transmission probability.

A. Complex absorbing potentials

The complex potentials not only absorb the outgoing waves but can also produce reflections themselves. The construction and optimization of reflection-free CAPs are therefore pursued by many research groups. Many different forms of pure imaginary potential have been investigated, including linear,[27] power-law,[28,30] polynomial,[31] and other parametrized functional forms (see Ref. 29 for a recent review). Besides purely imaginary potentials, complex potentials have also been investigated.[32] In this work we will adopt the CAP developed in Ref. 33 and refined in Ref. 34. This negative imaginary CAP is derived from a physically motivated differential equation and its form is[34]

$$-iw(x) = -i\frac{\hbar^2}{2m}\left(\frac{2\pi}{\Delta x}\right)^2 f(y), \tag{1}$$

where x_1 is the start and x_2 is the end of the absorbing region, $\Delta x = x_2 - x_1$, c is a numerical constant, m is the electron's mass, and

$$f(y) = \frac{4}{(c-y)^2} + \frac{4}{(c+y)^2} - \frac{8}{c^2}, \quad y = \frac{c(x-x_1)}{\Delta x}. \tag{2}$$

This CAP goes to infinity at the end of the absorbing region and is therefore exactly transmission free. The CAP contains only one parameter, the width of the absorbing region Δx. Its reflection properties are guaranteed to improve as this parameter is increased. Figure 2 shows the above CAP together with electron density calculated solving a one-dimensional model, scattering on a potential step. In the middle region, where the CAP is zero, the calculated and exact densities are equal. In the asymptotic region the wave function is absorbed by the CAP and the density gradually decreases to zero.

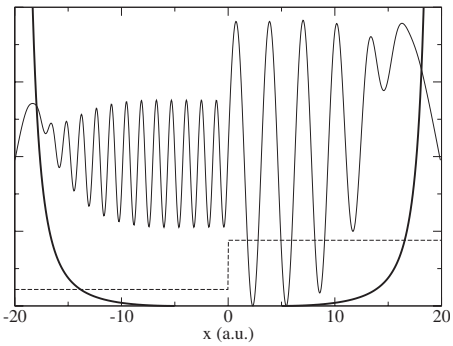

FIG. 2. Scattering on a potential step. The bold line shows the complex absorbing potential, the dashed line is the potential step, and the thin solid line is the square of the scattering wave function. In the middle region where the CAP is zero the wave function is in perfect agreement with the exact wave function (not shown in the figure).

B. Self-energies of the leads

To make the paper self-contained we briefly introduce the definition of self-energies used in transport calculations. In a suitably chosen basis representation the Hamiltonian and the overlap matrix of the left-lead–device–right-lead system (see Fig. 1), under the assumption that there is no interaction between the leads, takes the form

$$H = \begin{pmatrix} H_L & H_{LC} & 0 \\ H_{LC}^\dagger & H_C & H_{RC}^\dagger \\ 0 & H_{RC} & H_R \end{pmatrix}, \quad O = \begin{pmatrix} O_L & O_{LC} & 0 \\ O_{LC}^\dagger & O_C & O_{RC}^\dagger \\ 0 & O_{RC} & O_R \end{pmatrix}, \tag{3}$$

where H_L (O_L), H_C (O_C), and H_R (O_R) are the Hamiltonian (overlap) matrices of the leads and the device, and H_{LC} (O_{LC}) and H_{RC} (O_{RC}) are the coupling matrices between the central region and the leads. By defining the self-energies of the leads ($X=L,R$) as

$$\Gamma_X(E) = i[\Sigma_X(E) - \Sigma_X^\dagger(E)], \tag{4}$$

$$\Sigma_X(E) = (EO_{XC} - H_{XC})g_X(E)(EO_{XC} - H_{XC}), \tag{5}$$

where

$$g_X(E) = (EO_X - H_X)^{-1} \tag{6}$$

is the Green's function of the semi-infinite leads, and defining the Green's function of the central region

$$G_C(E) = [EO_C - H_C - \Sigma_L(E) - \Sigma_R(E)]^{-1}, \tag{7}$$

the transmission probability is given by

$$T(E) = \mathrm{Tr}[G_C(E)\Gamma_L(E)G_C^\dagger(E)\Gamma_R(E)]. \tag{8}$$

To calculate the transmission probability, one first has to calculate the Green's functions of the leads $g_L(E)$ and $g_R(E)$ for a given set of energy values and then determine the self-energies and the Green's function of the central region $G(E)$. The self-energy of the lead is usually calculated by assuming that the lead is made of periodically repeated blocks (see Fig. 1) and that the basis functions in these blocks only overlap between neighboring blocks.

C. Self-energies of the leads with CAP

By adding the CAP [as defined in Eq. (1)] to the Hamiltonian of the leads one obtains

$$H'_L = H_L - iW_L(x), \quad H'_R = H_R - iW_R(x), \tag{9}$$

where W_L and W_R are the matrix elements of the complex potential on the left and the right. Assuming that the basis states only connect the neighboring blocks in the lead, these matrices will have the same block-tridiagonal structure as the lead's Hamiltonian

$$H_R = \begin{pmatrix} h_R^{00} & h_R^{10\dagger} & 0 & 0 \\ h_R^{10} & h_R^{00} & h_R^{00\dagger} & 0 \\ 0 & h_R^{10} & h_R^{00} & \cdots \\ 0 & 0 & \cdots & \cdots \end{pmatrix}, \tag{10}$$

but for the nonperiodic complex potential the matrices in the diagonals will not be identical

$$W_R = \begin{pmatrix} w_R^{00} & w_R^{10\dagger} & 0 & 0 \\ w_R^{10} & w_R^{11} & w_R^{21\dagger} & 0 \\ 0 & w_R^{21} & w_R^{22} & \cdots \\ 0 & 0 & \cdots & \cdots \end{pmatrix}. \tag{11}$$

These are finite-dimensional Hamiltonians; beyond the range of the complex potential, the lead is effectively cut off. To simplify the calculations we assume that the complex potential starts one block away from the central region on both sides of the central region. With this choice, assuming that the basis functions in the leads only connect neighboring blocks, H_{LC} and H_{RC} will not contain contributions from the complex potential. The Hamiltonian of the system is now

$$H' = \begin{pmatrix} H'_L & H_{LC} & 0 \\ H_{LC}^\dagger & H_C & H_{RC}^\dagger \\ 0 & H_{RC} & H'_R \end{pmatrix}. \tag{12}$$

The transmission probability, the Green's function of the central region, and other quantities can be calculated in the same way as before by replacing the leads' Green's functions in the self-energies in Eq. (5) by

$$g'_X(E) = (EO_X - H'_X)^{-1}. \tag{13}$$

In passing we note that using simple algebra one can show that the transmission probability can also be calculated by using

$$T(E) = \mathrm{Tr}[G'(E)W_L G'^\dagger(E)W_R], \tag{14}$$

where

$$G'(E) = (EO - H')^{-1}. \tag{15}$$

This is the transmission probability formula used in quantum chemical reaction-rate calculations.[26] It differs from Eq. (8) in two ways: Γ is replaced by W and instead of the Green's function of the central region G_C it contains the Green's function G' of the whole system (including the complex potentials). This form, however, is computationally more expensive as the size of the G' matrix is larger than that of G_C.

By adding the complex potential to the Hamiltonian of the lead the semi-infinite Hamiltonian is transformed into a finite Hamiltonian. The simplest way to calculate Green's functions of the leads is to diagonalize the complex Hamiltonians H'_L and H'_R,

$$H'_X C_X = E_X O_X C_X, \quad (X = L,R). \tag{16}$$

The Green's function of the leads now can be calculated by the spectral representation

$$(g_L)_{ij} = \sum_k \frac{C_{Xik} C_{Xjk}}{E - E_{Xk}}, \tag{17}$$

where C_{Xik} is the ith component of the kth eigenvector belonging to eigenvalue E_{Xk}. As the Hamiltonian matrix of the lead is complex symmetric, the left and right eigenvalues are equal and the left and right eigenvectors are complex conjugates of each other. For a given lead this diagonalization only has to be done once in the beginning of the calculations and the self-energies are then available for any desired energy. The Hamiltonian and overlap matrices of the leads are in block-tridiagonal form and this special sparse property allows efficient iterative diagonalization. If the size of the eigenvalue problem becomes too large then one has to calculate the Green's function by direct inversion. This can also be efficiently done as shown in the Appendix. Another possibility is to calculate only the eigensolutions whose contribution dominate the spectral representation and introduce some effective truncation procedure.

III. RESULTS

In this section we show our test calculations for different systems. To demonstrate the effectiveness of our approach we have calculated the Green's functions of the leads by decimation[22] and by using the CAP approach and compared the transmission probabilities obtained by using the two different methods. As the CAP approach only affects the Green's functions of the leads, the device part is irrelevant and we have restricted our calculations to simple devices and tested the accuracy of the method for various leads.

A. Basis functions

In these tests we used DFT to describe the electronic structure of the leads and the device. We first calculated the self-consistent potential in the leads and in the device and then set up the Hamiltonian and overlap matrices. The DFT calculation was implemented on the Lagrange function basis.[38] We define three sets of Lagrange basis functions φ_i^L and φ_i^R for the periodically repeated block in the left and the right leads and φ_i^C for central region. The basis functions are allowed to overlap with the neighboring blocks but only with the nearest neighbors. In practice that means that the Lagrange basis grid extends into the neighboring block in the left and in the right. Next, using these basis functions we have diagonalized the Hamiltonian of the central region H_C and the Hamiltonians h_L and h_R of the periodically repeated blocks. Using an energy cutoff E_c we have truncated the

eigenfunction sets. The eigenfunction sets ϕ_i^L, ϕ_i^R, and ϕ_i^C with eigenenergies below the energy cutoff are used as basis states in the calculation.

Using the basis sets constructed as described above, the matrix elements of the Hamiltonian in the central region are defined as

$$(H_C)_{ij} = \langle \phi_i^C | H | \phi_j^C \rangle, \quad (H_{XC})_{ij} = \langle \phi_i^X | H | \phi_j^C \rangle, \tag{18}$$

where $X=L,R$. The Hamiltonians of the lead parts are

$$(h_X)_{ij}^{00} = \langle \phi_i^X | H | \phi_j^X \rangle, \quad (h_X)_{ij}^{10} = \langle \phi_i^{X'} | H | \phi_j^X \rangle, \tag{19}$$

with

$$\phi^{X'}(x,y,z) = \phi^X(x+a,y,z), \quad (a=l,r), \tag{20}$$

where l and r are the distances between the centers of the periodically repeated blocks in the leads. The overlap matrix is defined analogously by replacing H with the unit operator. These basis functions thus connect only the nearest-neighbor blocks leading to block-tridiagonal matrix representations. This allows us to use the decimation technique to calculate the leads' self-energies and compare the results to those obtained by the CAP approach.

A similar block-tridiagonal structure could have been achieved by employing atomic-orbital type basis functions provided that the cutoff radius of the atomic orbitals and the size of the periodically repeated blocks are suitably chosen. Other choices of basis functions are also possible. The main motivation behind the Lagrange function representation was the simplicity of the implementation.

The energy cutoff E_c is chosen in such a way that the maximum change in the transmission probability due to the increase of E_c is smaller than 1%. The typical number of basis states used in the calculations is about 3–4 times of the number of electrons in a given block.

B. Conductance of monoatomic aluminum wire

Our first example is a monoatomic Al wire (placing Al atoms 2.4 Å apart). Both the decimation and the CAP approaches use the same basis and therefore, apart from the complex potential in the CAP case, the Hamiltonian and overlap matrices are identical. The decimation provides well converged self-energies after about 25 iterations and we consider this the "exact" results and compare it to the CAP results. Figure 3 shows the convergence of the CAP results for different ranges of the complex potential (in units of number of lead blocks). As mentioned earlier, the increase of the CAP range leads to the decrease of reflections and the CAP results quickly converge to the exact values. In the CAP approach, the leads' Green's functions were expressed by their spectral representation, so after the eigenvalue problem [Eq. (16)] was solved the self-energies were available for any energy at no extra cost.

We also tested the direct inversion (described in the Appendix) which has to be repeated for all energies of interest. Both methods give identical results. Table I compares the calculation time for the different approaches. The direct inversion is about ten times faster than decimation and in larger lead blocks the speed up is expected to be even more significant. The computational times presented in the table are the times spent for calculating the self-energy for 100 energy values. In case of CAP with diagonalization, this time is essentially spent on the diagonalization of the leads' complex Hamiltonians and adding more energy values does not change the computational time. In both decimation and CAP with direct inversion, the computational time is directly proportional to the number of energy values.

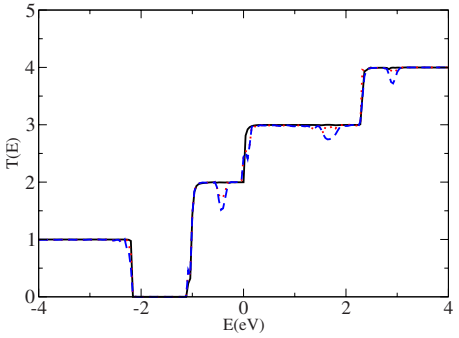

FIG. 3. (Color online) Transmission probability of a monoatomic Al wire. The result obtained by the decimation method (solid black line) is compared to the CAP of different ranges (blue dashed line two blocks, red dotted line four blocks). The CAP results using six blocks are indistinguishable from the decimation results within the line width on the figure.

C. Conductance of monoatomic C wire between Al leads

The calculation of the conductance of a monoatomic carbon wire is a popular test case of transport calculations.[39–41] In this test case a straight wire of seven carbon atoms is attached to Al(100) electrodes (lattice constant 4.05 Å). The C-C distance is fixed to 1.42 Å and the distance between the ends of the carbon chain and the first plane of Al atoms is 1 Å. The Al lead block contains 18 atoms in four layers. The blocks in the right and the left lead are identical.

Figure 4 shows the transmission probability as a function of the energy. The CAP and decimation results are in complete agreement.

D. Conductance of carbon nanotubes

In this example we calculated the conductance of carbon nanotubes and compared the transmission obtained from

TABLE I. Basis size and computational time of the presented examples. $N_L=N_R$ is the dimension of the basis representing the lead block. The calculation time (in seconds) is the calculation time of the self-energy for 100 energy values using CAP with diagonalization (CAP1), CAP with direct inversion (CAP2), and decimation.

System	N_L	CAP1	CAP2	Decimation
Al mono	30	0.05	0.6	5.1
Al wire	180	10.0	130	1230
CN (10,10)	300	45	580	6870

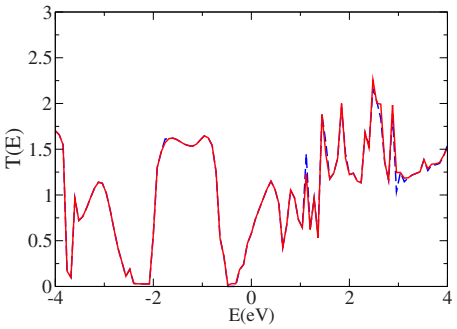

FIG. 4. (Color online) Transmission probability of a seven-atom monoatomic C wire sandwiched between Al(100) electrodes. The result obtained by the decimation method (solid red line) is compared to the CAP result (dashed blue line) obtained by using six lead blocks.

CAP and decimation. The agreement between the two approaches (Fig. 5) is again excellent. Next, we test the CAP method for a carbon nanotube with a Hückel Hamiltonian. The tight-binding matrix elements are taken from Ref. 42 and the parametrization used is from Ref. 43. In this case, we did not explicitly calculate the matrix elements of the complex potentials but in the spirit of the Hückel approach we simply added the $W(x)$ to the diagonal elements of the Hamiltonian. [The complex potential $W(x)$ was evaluated at the corresponding atomic positions.] The results are shown in Fig. 6. In this case, the agreement is not perfect, but considering the approximate nature of the construction of the matrix elements the closeness of the results is remarkable.

IV. SUMMARY

We have presented an efficient and accurate way to calculate self-energy matrices of the Green's function calculations. By adding a complex absorbing potential to the Hamiltonian of the semi-infinite lead, the lead can be terminated in a finite distance leading to finite-dimensional matrices. In this way the leads' Green's functions can be calculated from their spectral representation for any energy at once. The test examples presented in the paper show the accuracy and effectiveness of the approach. For a given lead and basis set the lead's Green's functions can be precalculated and tabulated eliminating the computational bottleneck related to self-energy evaluations in transport calculations.

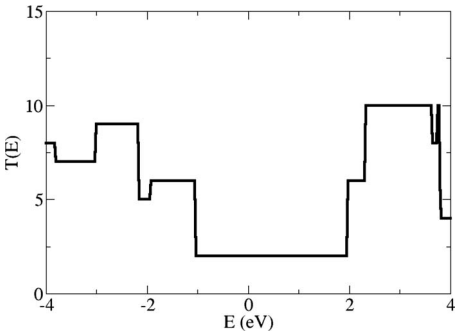

FIG. 5. Transmission probability of a (10,10) carbon nanotube. The decimation and CAP (six blocks) results are in perfect agreement.

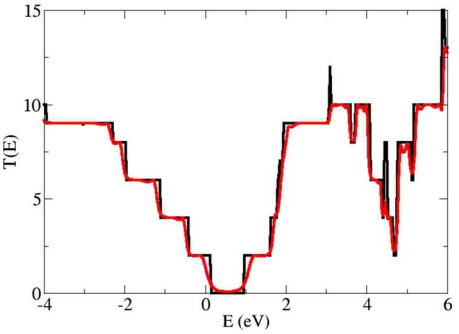

FIG. 6. (Color online) Transmission probability of a (5,5) carbon nanotube using Huckel Hamiltonian. The CAP calculation is obtained by using six blocks.

We have used a CAP which depends only on one parameter, its range and its accuracy can be increased by enlarging the range. This gives us a very effective way of controlling the convergence of the method. Other choices of complex potentials are possible; we will work on optimizing the CAP for transport calculations.

In typical transport calculations the dimension of the matrices used to describe a single block of the lead is on the order of a few hundreds. In our approach 4–6 of those blocks are used so the typical dimension of the matrices to be diagonalized is a few hundreds to a few thousands. Complex symmetric matrices of that size can be easily diagonalized with standard direct diagonalization approaches. The Hamiltonian and overlap matrices are block tridiagonal, and by using this special sparse structure the diagonalization can be made much faster. Iterative diagonalization can also be useful but so far we have used the whole eigenspectrum to construct the Green's functions, and so the advantage of iterative approaches when more than a few eigensolutions is needed is not tested. In the future we will investigate the possibility of using only a few dominant eigensolutions in the spectral representation of the leads' Green's functions. If a few dominant eigensolutions provide satisfactory accuracy, an iterative solution for those target eigensolutions will make the approach even more powerful.

The present work implemented the CAP approach using basis states that only connect the neighboring blocks in the lead. This choice was made to allow direct comparison between the decimation method and the CAP approach and test the accuracy of the latter. The CAP can be implemented with other basis function representations as well. Work in that direction will be pursued in the future.

ACKNOWLEDGMENTS

This work was supported by NSF under Grant No. ECS-0622146.

APPENDIX

If the size of the eigenvalue problem in Eq. (16) becomes unmanageable by iterative methods, one has to calculate the

inverse directly. For completeness, we provide an algorithm to perform this inverse. The calculated part of the lead's Green's function that enters into self-energy matrices has block-tridiagonal form, and the algorithm takes advantage of this structure. The function $g'_X(E)$ is used only in Eq. (5), and in that context only the first $(X=L)$ or last $(X=R)$ of the N diagonal blocks of $g'_X(E)$ is needed. The calculation of the ith diagonal block of $g'_X(E)$ is given by

$$g'_{Xi} = (A_i - B_i)^{-1}, \tag{A1}$$

where A_i and B_i are calculated recursively as

$$A_i = h_X^{00} - h_X^{10} A_{i+1}^{-1} h_X^{01}, \quad A_N = h_N^{00}, \tag{A2}$$

$$B_i = h_X^{01}(h_X^{00} - B_{i-1})^{-1} h_X^{10}, \quad B_1 = 0, \tag{A3}$$

where

$$h_X^{00}(E) = Eo_X^{00} - h_X^{00} + iw_X^{00}, \tag{A4}$$

$$h_X^{01}(E) = Eo_X^{01} - h_X^{01} + iw_X^{01}, \tag{A5}$$

$$h_X^{10} = h_X^{01}. \tag{A6}$$

[1] L. P. Kadanoff and G. Baym, *Quantum Statistical Mechanics* (Benjamin, New York, 1962); L. V. Keldysh, Sov. Phys. JETP **20**, 1018 (1965).
[2] S. Datta, *Electronic Transport in Mesoscopic Systems* (Cambridge University Press, Cambridge, 1997).
[3] M. DiVentra, *Electrical Transport in Nanoscale Systems* (Cambridge University Press, Cambridge, 2008).
[4] S. V. Faleev, F. Leonard, D. A. Stewart, and M. van Schilfgaarde, Phys. Rev. B **71**, 195422 (2005).
[5] J. J. Palacios, A. J. Perez-Jimenez, E. Louis, E. SanFabian, and J. A. Verges, Phys. Rev. Lett. **90**, 106801 (2003).
[6] K. Stokbro, J. Taylor, M. Brandbyge, J.-L. Mozos, and P. Ordejon, Comput. Mater. Sci. **27**, 151 (2003).
[7] E. G. Emberly and G. Kirczenow, Phys. Rev. B **64**, 235412 (2001).
[8] J. Taylor, H. Guo, and J. Wang, Phys. Rev. B **63**, 245407 (2001).
[9] M. B. Nardelli, J.-L. Fattebert, and J. Bernholc, Phys. Rev. B **64**, 245423 (2001).
[10] Y. Xue, S. Datta, and M. A. Ratner, J. Chem. Phys. **115**, 4292 (2001).
[11] K. S. Thygesen and K. W. Jacobsen, Chem. Phys. **319**, 111 (2005).
[12] S.-H. Ke, H. U. Baranger, and W. Yang, Phys. Rev. B **70**, 085410 (2004).
[13] P. A. Derosa and J. M. Seminario, J. Phys. Chem. B **105**, 471 (2001).
[14] A. Zhang, L. Fonseca, and A. A. Demkov, Phys. Status Solidi B **233**, 70 (2002).
[15] S. Sanvito, C. J. Lambert, J. H. Jefferson, and A. M. Bratkovsky, Phys. Rev. B **59**, 11936 (1999).
[16] M. Di Ventra, S. T. Pantelides, and N. D. Lang, Phys. Rev. Lett. **84**, 979 (2000).
[17] P. A. Khomyakov and G. Brocks, Phys. Rev. B **70**, 195402 (2004).
[18] R. Gebauer, K. Burke, and R. Car, Lect. Notes Phys. **706**, 463 (2006).
[19] G. Stefanucci and C.-O. Almbladh, Phys. Rev. B **69**, 195318 (2004).
[20] G. Stefanucci, S. Kurth, E. K. U. Gross, and A. Rubio, *Molecular and Nano Electronics: Analysis, Design and Simulation*, Elsevier Series on Theoretical and Computational Chemistry, edited by J. Seminario (Elsevier, New York, 2007), Vol. 17, p. 247.
[21] J. Velev and W. Butler, J. Phys.: Condens. Matter **16**, R637 (2004).
[22] M. P. Lopez Sancho, J. M. Lopez Sancho, J. M. L. Sancho, and J. Rubio, J. Phys. F: Met. Phys. **15**, 851 (1985).
[23] T. Ando, Phys. Rev. B **44**, 8017 (1991).
[24] P. S. Krstic, X.-G. Zhang, and W. H. Butler, Phys. Rev. B **66**, 205319 (2002).
[25] R. Kosloff and D. Kosloff, J. Comput. Phys. **63**, 363 (1986).
[26] W. H. Miller, Acc. Chem. Res. **26**, 174 (1993) and references therein.
[27] M. S. Child, Mol. Phys. **72**, 89 (1991).
[28] T. Seideman and W. H. Miller, J. Chem. Phys. **96**, 4412 (1992).
[29] J. G. Muga, J. P. Palao, B. Navarro, and I. L. Egusquiza, Phys. Rep. **395**, 357 (2004).
[30] A. Vibok and G. G. Balint-Kurti, J. Phys. Chem. **96**, 8712 (1992).
[31] S. Brouard, D. Macias, and J. G. Muga, J. Phys. A **27**, L439 (1994).
[32] G. Jolicard and J. Humbert, Chem. Phys. **118**, 397 (1987).
[33] D. E. Manolopoulos, J. Chem. Phys. **117**, 9552 (2002).
[34] T. Gonzalez-Lezena, E. J. Rackham, and D. E. Manolopoulos, J. Chem. Phys. **120**, 2247 (2004).
[35] X.-G. Zhang, K. Varga, and S. T. Pantelides, Phys. Rev. B **76**, 035108 (2007).
[36] K. Varga and S. T. Pantelides, Phys. Rev. Lett. **98**, 076804 (2007).
[37] T. M. Henderson, G. Fagas, E. Hyde, and J. C. Greer, J. Chem. Phys. **125**, 244104 (2006).
[38] K. Varga, Z. Zhang, and S. T. Pantelides, Phys. Rev. Lett. **93**, 176403 (2004).
[39] M. Brandbyge, J.-L. Mozos, P. Ordejon, J. Taylor, and K. Stokbro, Phys. Rev. B **65**, 165401 (2002).
[40] N. D. Lang and P. Avouris, Phys. Rev. Lett. **84**, 358 (2000).
[41] B. Larade, J. Taylor, H. Mehrez, and H. Guo, Phys. Rev. B **64**, 075420 (2001).
[42] J. C. Slater and G. F. Koster, Phys. Rev. **94**, 1498 (1954).
[43] J. C. Charlier, P. Lambin, and T. W. Ebbesen, Phys. Rev. B **54**, R8377 (1996).